

Laser-induced magnetization precession in individual magnetoelastic domains of a multiferroic CoFeB/BaTiO₃ composite

L. A. Shelukhin,^{1,*} N. A. Pertsev,¹ A. V. Scherbakov,^{1,2} D. L. Kazenwadel,³
D. A. Kirilenko,¹ S. J. Hämmäläinen,⁴ S. van Dijken,⁴ and A. M. Kalashnikova¹

¹*Ioffe Institute, 194021 St. Petersburg, Russia*

²*Experimental Physics II, Technical University Dortmund, D-44227 Dortmund, Germany*

³*University of Konstanz, D-78457 Konstanz, Germany*

⁴*NanoSpin, Department of Applied Physics, Aalto University School of Science, P.O. Box 15100, FI-00076 Aalto, Finland*

(Dated: March 26, 2025)

Using a magneto-optical pump-probe technique with micrometer spatial resolution we show that magnetization precession can be launched in individual magnetic domains imprinted in a Co₄₀Fe₄₀B₂₀ (CoFeB) layer by elastic coupling to ferroelectric domains in a BaTiO₃ substrate. The dependence of the precession parameters on external magnetic field strength and orientation reveals that laser-induced ultrafast partial quenching of the magnetoelastic coupling parameter of CoFeB by $\sim 15\%$ along with 5% ultrafast demagnetization trigger the magnetization precession. The relation between laser-induced reduction of the magnetoelastic coupling and the demagnetization can be well approximated by the $n(n+1)/2$ -law with $n=2$ corresponding to the uniaxial anisotropy, confirming the thermal origin of the laser-induced anisotropy change. The excitation process in an individual magnetoelastic domain is found to be unaffected by neighboring domains. This makes laser-induced changes of magnetoelastic anisotropy a promising tool for driving magnetization dynamics in composite multiferroics with spatial selectivity.

Magnetoelectric multiferroics offer a possibility to control magnetization by an electric field [1–3], which is in high demand for beyond CMOS technologies [4] including sensors, energy harvesters, memories and logic devices [5]. However, the number of single-phase multiferroics is limited [6], with many of the materials exhibiting multiferroic properties below room temperature or providing insufficient coupling between the order parameters. On the other hand, composite structures consisting of ferromagnetic (FM) and ferroelectric (FE) materials coupled via strain represent a promising alternative for achieving indirect magnetoelectric coupling at room temperature of sufficient strength for future applications [5, 7–10].

In strain-coupled composite multiferroics, the magnetic anisotropy of the FM is altered by a combination of interfacial strain transfer from the FE and inverse magnetostriction. For properly selected FM and FE materials, heterostructure geometries, and optimized interfaces, strong magnetization responses to external electric fields can be obtained. In particular, full imprinting of ferroelastic domain patterns from FE substrates into FM overlayers with in-plane and perpendicular magnetizations and their subsequent manipulation by electric fields have been demonstrated experimentally [11–17]. FM-FE composites enable electric-field-induced magnetization switching leading to changes in magnetoresistance [18–22], electrical tuning of ferromagnetic resonance and spin-wave spectra [23–26], active filtering and routing of propagating spin waves [27, 28], and electrical switching between superconducting and normal states [29].

Control over the order parameters of composite multiferroic structures by femtosecond laser pulses would widen their application perspectives and elevate their switching speed. There are several pathways along which an ultrafast optical stimulus may alter the state of a com-

posite multiferroic. One relies on ultrafast direct optical control of magnetization [30] and, via FM-FE coupling, of ferroelectric polarization [31, 32]. Alternatively, ultrafast optically-driven changes of the FE state could lead to high-amplitude dynamical strain modulations [33] and, thus, alter the magnetization state of a magnetostrictive layer. However, ultrafast optical control of FE polarization remains challenging [34]. Optically-induced strain as a tool to modify the anisotropy of a FM in FM-photostrictive composites is considered in [35], but results reported thus far do not extend to ultrafast timescales.

In this Letter, we examine an alternative approach to ultrafast optical control of a composite multiferroic, and study the feasibility of ultrafast laser-induced changes of strain-mediated magnetoelectric coupling in a CoFeB/BaTiO₃ heterostructure. Using a femtosecond magneto-optical pump-probe technique with micrometer spatial resolution, we excite magnetization precession in individual magnetic domains imprinted in the amorphous CoFeB layer by mechanical coupling to ferroelastic domains in BaTiO₃. We reveal that the precession is triggered by an abrupt decrease of the CoFeB magnetoelastic coupling parameter and magnetization by $\sim 15\%$ and 5% , respectively, for an incident laser pulse fluence of 10 mJ/cm^2 . This ratio satisfies the $n(n+1)/2$ -law with $n=2$ that describes the temperature-induced variations of a single-ion uniaxial magnetic anisotropy, confirming the thermal origin of the observed changes.

The heterostructure under study consists of a 50-nm-thick layer of a FM CoFeB amorphous alloy on a 500- μm -thick single-crystalline BaTiO₃ (001) substrate (see Suppl. Mater. for a transmission electron microscopy image). CoFeB layer is grown on BaTiO₃ by magnetron sputtering at $T_g = 573 \text{ K}$ and capped with a 6-nm-thick Au layer. At room temperature (RT), the BaTiO₃

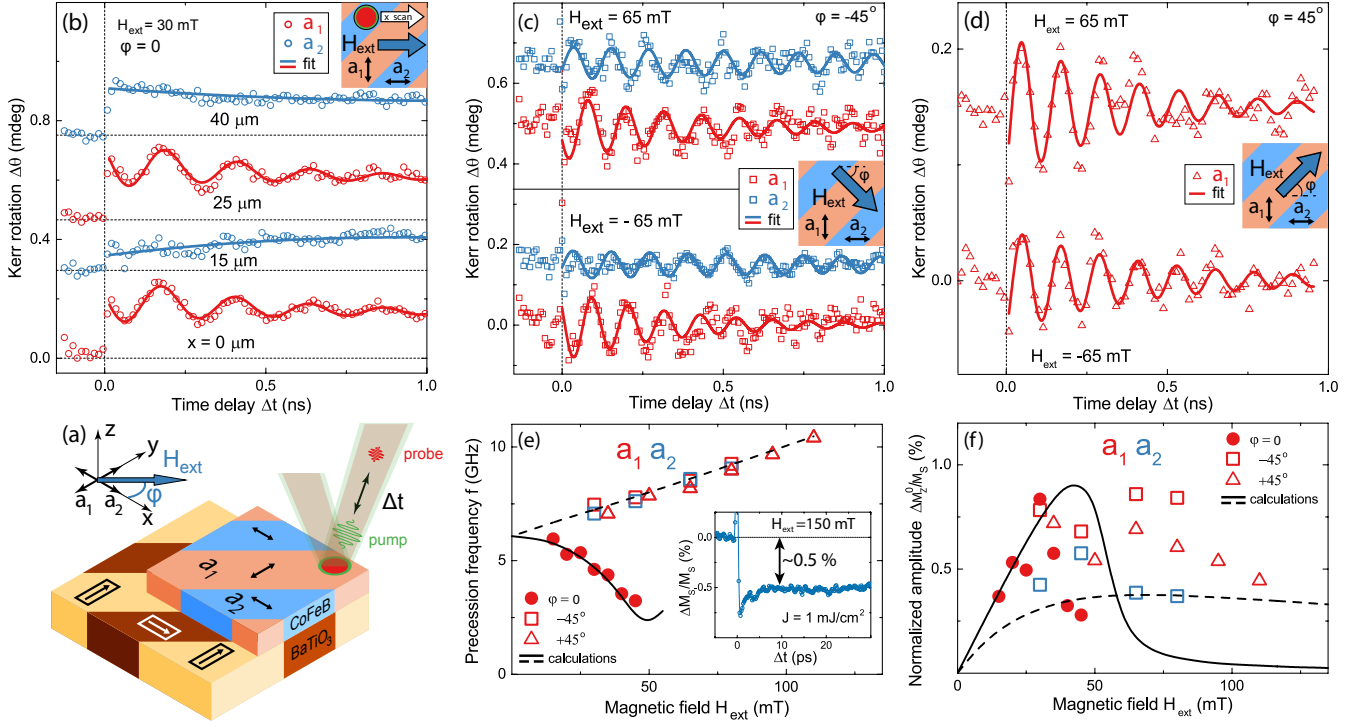


FIG. 1. (Color online) (a) Schematics of the CoFeB/BaTiO₃ structure and the pump-probe experiment. Arrows in rectangles and double-headed arrows indicate the spontaneous polarization in the ferroelastic domains of BaTiO₃ and the strain-induced magnetic anisotropy axes of the a₁ and a₂ domains in the CoFeB layer, respectively. (b-d) Laser-induced Kerr rotation $\Delta\theta$ of the probe pulse polarization as a function of time delay Δt measured in a₁ (red symbols) or a₂ (blue symbols) domains. The external magnetic field \mathbf{H}_{ext} is applied at (b) $\varphi = 0$, (c) $\varphi = -45^\circ$, and (d) $\varphi = 45^\circ$. In (c,d) the signals measured at positive (upper curves) and negative (lower curves) H_{ext} are shown. Lines are fits to the measurement data (see text). (e,f) Experimental magnetic field dependencies of (e) the values of precession frequency f and (f) the normalized amplitude $\Delta M_z^0/M_S$ in the a₁ (red symbols) and a₂ (blue symbols) domains at $\varphi = 0$ (solid circles), $\varphi = -45^\circ$ (open squares), and $\varphi = 45^\circ$ (triangles). Solid and dashed lines are the calculated dependencies for the a₁ domain for $\varphi = -1^\circ$ and $\varphi = -45^\circ$, respectively. The inset in panel (e) shows the ultrafast demagnetization measured at a pump fluence of 1 mJ/cm² and $H_{\text{ext}} = 150$ mT.

substrate is split into 90° ferroelectric-ferroelastic stripe domains with in-plane spontaneous polarization aligned along the long side of the tetragonal unit cell [12]. Owing to the strain transfer from BaTiO₃ to CoFeB and inverse magnetostriction, an uniaxial magnetoelastic anisotropy is locally induced in the CoFeB film. Since the magnetostriction parameter λ of CoFeB is positive, the magnetic anisotropy easy axes are oriented parallel to the polarizations of the underlying FE domains [12, 14] [Fig. 1 (a)]. The strain-induced magnetoelastic anisotropy dominates over other anisotropy contributions, and the stripe domain patterns in CoFeB and BaTiO₃ fully correlate. The two types of stripe domains a₁ and a₂ have widths of $\sim 12\mu\text{m}$ and $\sim 3\mu\text{m}$, respectively.

Laser-induced dynamics of the magnetization in distinct magnetic domains in the CoFeB/BaTiO₃ composite is studied using a femtosecond two-color magneto-optical pump-probe setup. The pump and probe pulse durations are 170 fs, and the central wavelengths of the pump and probe pulses are 515 nm and 1030 nm, respectively. The pump pulse fluence is 10 mJ/cm², while the probe pulse fluence is ~ 10 times lower. Both pump and probe pulses

are focused on the CoFeB layer into a spot with a diameter below 5 μm using a 15x reflective microscope objective. The laboratory frame is chosen such that the x , y , and z axes are directed along the easy axes of the a₂, a₁ domains and the sample normal, respectively [Fig. 1(a)]. An external DC magnetic field \mathbf{H}_{ext} of strength 0–120 mT is applied in the sample plane at an angle φ to the x axis. Measurements of laser-induced magnetization dynamics at $\varphi = 0, \pm 45^\circ$ in a₁ and a₂ domains are performed by displacing the sample laterally with 0.05 μm precision. The pump-induced changes of magnetization are traced by recording the magneto-optical Kerr rotation $\Delta\theta$ of the probe polarization plane as a function of time delay Δt between the pump and probe pulses. The incidence angle of the probe pulses is 17°, and the measured Kerr rotation $\Delta\theta(\Delta t)$ is proportional mostly to the pump-induced changes of the out-of-plane component M_z of magnetization. All measurements are performed at RT.

Figure 1(b) shows the laser-induced probe polarization rotation $\Delta\theta(\Delta t)$ measured for different positions x of laser spots on the sample surface. The external magnetic field \mathbf{H}_{ext} is parallel (perpendicular) to the easy

axis of the a_2 (a_1) domain ($\varphi = 0$). At $H_{\text{ext}} = 30$ mT one clearly distinguishes two types of dynamic signal $\Delta\theta(\Delta t)$ depending on x . At $x = 0$ and $25 \mu\text{m}$ clear oscillations of $\Delta\theta$ are observed, while at $x = 15$ and $40 \mu\text{m}$ only a slowly varying change of $\Delta\theta$ is seen. Detailed studies of $\Delta\theta(\Delta t)$ at $x = 0$ for different magnetic field strengths reveal that the oscillatory signal is present only in the range of 0–45 mT. The amplitude and the frequency of the oscillations as a function of the applied magnetic field were obtained by fitting the signal at $x = 0$ to the function $\Delta\theta(\Delta t) = \Delta\theta_0 \exp(-t/\tau_d) \sin(2\pi f t + \xi_0) + P_2(t)$, where $\Delta\theta_0$, f , ξ_0 , τ_d are the oscillation amplitude, frequency, initial phase, and decay time, respectively. The second-order polynomial function $P_2(t)$ accounts for a slowly varying background of nonmagnetic nature. The field dependence of the frequency f [Fig. 1(e)] resembles that of a magnetization precession in a field applied perpendicularly to the easy axis. Therefore, the signal at $x = 0$ can be confidently ascribed to the laser-induced precession of magnetization in the a_1 domain. The periodicity and the width of the areas in which laser-induced precession is detected (at $x = 0, 25 \mu\text{m}$) and not detected (at $x = 15, 40 \mu\text{m}$) correspond to the length scale of the magnetic domain pattern in the sample. In order to relate $\Delta\theta_0$ to the amplitude ΔM_z^0 of variations of the out-of-plane magnetization component, the measurement signal was normalized by the static magneto-optical Kerr rotation angle at saturation $\theta_S = 10$ mdeg, which is proportional to the saturation magnetization M_S . The field dependence of $\Delta M_z^0/M_S$ is shown in Fig. 1(f).

If the external field \mathbf{H}_{ext} is applied at an angle $\varphi = -45^\circ$, i.e., if it makes an angle of $\pm 45^\circ$ to the easy axes of the a_1 and a_2 domains, a laser-induced precession is observed in both stripe domains in a wider field range. Fig. 1(c) shows $\Delta\theta(\Delta t)$ measured in the a_1 (red dots) and the a_2 (blue dots) domains at $H_{\text{ext}} = \pm 65$ mT. As one can see, upon the transition from the a_1 to the a_2 domain the initial phase ξ_0 of the magnetization precession changes by 180° . Reversal of the magnetic field sign, in turn, does not affect the character of the excited precession. The dependence of the precession frequency on field strength [Fig. 1(e)] is typical for a geometry wherein the field is applied at 45° with respect to the uniaxial magnetic anisotropy axis and is the same for both domains. The precession amplitude shows small variations with applied field strength and is somewhat higher in the wider a_1 domain [Fig. 1(f)]. When the external field is applied at $\varphi = 45^\circ$, a laser-induced precession is detected in the a_1 domains only [Fig. 1(c)]. The field dependencies of the precession frequency and amplitude are similar to those found in the a_1 domains at $\varphi = -45^\circ$ [Fig. 1(e,f)].

The magnetization precession in the individual domains excited at $\varphi = 0, -45^\circ$ agrees well with the general scenario of laser-induced changes of magnetic anisotropy [36, 37]. As discussed in detail in e.g. [38, 39], a fast change of the effective anisotropy field produces a magnetization precession. The efficiency of excitation is highly sensitive to the alignment of equilibrium magnetization

with respect to the easy anisotropy axis. In our experiments, the magnetization precession in a particular domain is not excited when the external field is aligned along the easy anisotropy axis of the domain [Fig. 1(b)]. When the field is aligned perpendicularly to the easy anisotropy axis of the domain, the precession is excited only if the field strength is below the anisotropy field. The latter is easily identified in our experiments as the field at which the frequency of the precession is minimal [Fig. 1(e)]. Finally, when the magnetic field is at an intermediate angle to the easy anisotropy axis, e.g. at $\pm 45^\circ$, the magnetization precession is excited in a wider field range [Fig. 1(e, f)].

The light penetration depth in the CoFeB layer is below 20 nm at the pump wavelength of 515 nm, and, therefore, we argue that the anisotropy changes are caused by laser-induced processes in the FM film but not by changes in the FE substrate. In contrast to metallic films with a pronounced magnetocrystalline anisotropy considered in [36, 37] and following works, here the magnetic anisotropy of amorphous CoFeB film is fully dominated by an uniaxial magnetoelastic anisotropy. Hence magnetization-dependent part of the free energy density F in an individual domain contains only the Zeeman, magnetoelastic, and shape anisotropy terms [40]:

$$F = -\mu_0 \mathbf{M}_S \cdot \mathbf{H}_{\text{ext}} + B_1 (u_{xx} m_x^2 + u_{yy} m_y^2) + \left[\frac{1}{2} \mu_0 M_S^2 - \frac{c_{12}}{c_{11}} B_1 (u_{xx} + u_{yy}) \right] m_z^2, \quad (1)$$

where $m_i = M_i/M_S$, u_{xx} , u_{yy} are the substrate-induced in-plane strains in the CoFeB film, $B_1 = -1.5\lambda(c_{11} - c_{12})$ is the magnetoelastic coupling parameter, and $c_{11} = 2.8 \cdot 10^{11}$ N/m², $c_{12} = 1.4 \cdot 10^{11}$ N/m² are the elastic stiffnesses of CoFeB at constant magnetization \mathbf{M}_S taken to be those of Fe₆₀Co₄₀ [41]. The misfit strains u_{xx} and u_{yy} are expected to be fully relaxed at the growth temperature $T_g = 573$ K, which is well above the Curie temperature $T_C = 393$ K of BaTiO₃. On cooling from T_g , nonzero strains appear in the film owing to the difference in the thermal expansion coefficients of the paraelectric BaTiO₃ $\alpha_0 = 10 \cdot 10^6$ K⁻¹ [42] and CoFeB $\alpha_b = 12 \cdot 10^6$ K⁻¹ [43]. Taking into account that spontaneous strains appear in BaTiO₃ below T_C , we obtain $u_{xx}(T) = a(T)a_0(T_g)^{-1}[1 + \alpha_b(T - T_g)]^{-1} - 1$ and $u_{yy}(T) = c(T)a_0(T_g)^{-1}[1 + \alpha_b(T - T_g)]^{-1} - 1$ for the a_1 domain, and *vice versa* for the a_2 one. Here c , a , and a_0 are the lattice constants of the tetragonal FE and cubic paraelectric phases of BaTiO₃, respectively. We obtain $u_{xx} \approx -0.94\%$ and $u_{yy} \approx +0.79\%$ for the a_1 domain at RT by taking $c = 0.4035$ nm, $a = 0.3966$ nm [44], and $a_0(T_g) = 0.4017$ nm [45]. Additional in-plane anisotropy originating from the stripe shape of the domains has been shown to be negligible [12] and is not included in Eq. (1). The orientation of magnetization in the a_1 domain is given by the total effective field $\mathbf{H}_{\text{eff}} = -\mu_0^{-1} \partial F / \partial \mathbf{M}$, which is a sum of the external field \mathbf{H}_{ext} , the out-of-plane effective field $\mathbf{H}_{\text{out}} = [-M_S + 2B_1(\mu_0 M_S)^{-1}(u_{xx} + u_{yy})c_{11}c_{12}^{-1}] \mathbf{m}_z$,

and the effective magnetoelastic anisotropy field $\mathbf{H}_{\text{ME}} = -2B_1(\mu_0 M_S)^{-1}(u_{xx}\mathbf{m}_x + u_{yy}\mathbf{m}_y)$.

Excitation of the metallic CoFeB film by a femtosecond laser pulse results in a rapid increase of the temperatures of electronic and ionic systems, which equilibrate after several picoseconds. This yields, first of all, ultrafast demagnetization, i.e., a subpicosecond decrease ΔM_S of the saturation magnetization [46] followed by partial restoration upon equilibration between the lattice and electron temperatures [47]. Ultrafast demagnetization ΔM_S would increase the magnetoelastic anisotropy field $H_{\text{ME}} \propto M_S^{-1}$. However, a rapid rise of the film temperature following excitation by a laser pulse should also lead to a decrease ΔB_1 of the temperature-dependent magnetoelastic coupling parameter B_1 . In contrast to ultrafast demagnetization, this would reduce the effective magnetoelastic field $H_{\text{ME}} \propto B_1$. Finally, laser-induced heating ΔT modifies the substrate-induced film strains u_{xx} and u_{yy} via the term $\alpha_b \Delta T$ accounting for the thermal expansion of CoFeB, while the substrate temperature does not change significantly in our case. The resulting variations Δu_{xx} and Δu_{yy} could alter the in-plane field $\mathbf{H}_{\text{ME}} \propto (u_{xx}\mathbf{m}_x + u_{yy}\mathbf{m}_y)$ additionally. The changes ΔM_S , ΔB_1 and $\Delta u_{xx(yy)}$ affect the out-of-plane anisotropy field \mathbf{H}_{out} and launch precession if \mathbf{H}_{out} is nonzero in the initial state [48], which is not the case in our experiments.

In order to verify whether laser-induced changes of the in-plane magnetoelastic anisotropy can indeed account for the observed magnetization precession and to reveal which of the three contributions dominates, we performed numerical calculations. The precession frequency is governed by the external magnetic field, partially quenched magnetization, and modified magnetoelastic anisotropy within the laser excitation area and can be calculated using the Smit-Suhl formulas [49, 50]. The amplitude of the excited precession is defined by the azimuthal angle $\Delta\psi_{\text{eff}}$ by which the total effective field \mathbf{H}_{eff} reorients as a result of laser-induced changes ΔM_S , ΔB_1 , and $\Delta u_{xx(yy)}$. In the experiments, out-of-plane oscillations of magnetization are detected, and their amplitude can be found as $\Delta M_z^0/M_S = \epsilon \Delta\psi_{\text{eff}}$, where ϵ is the precession ellipticity [51].

The degree of ultrafast demagnetization $\Delta M_S/M_S$ in the studied sample is obtained experimentally by measuring the laser-induced rotation dynamics of the longitudinal magneto-optical Kerr rotation for the in-plane saturated sample [see inset in Fig. 1(e)]. At the laser fluence of 10 mJ/cm^2 , $\Delta M_S/M_S \approx -5\%$ at $\Delta t > 5 \text{ ps}$. Since a quasi-equilibrium between the electronic, ionic and spin systems establishes after several picoseconds following excitation, we assume that at $\Delta t > 5 \text{ ps}$ the laser-induced change of the magnetoelastic parameter B_1 relates to the demagnetization via the thermodynamic relation $B_1(T)/B_1(T=0) = [M_S(T)/M_S(T=0)]^{n(n+1)/2}$ [52]. For the uniaxial magnetoelastic anisotropy of the individual domains, we use $n = 2$ according to its single-ion origin [53, 54] and experimental data for Fe-Co-based

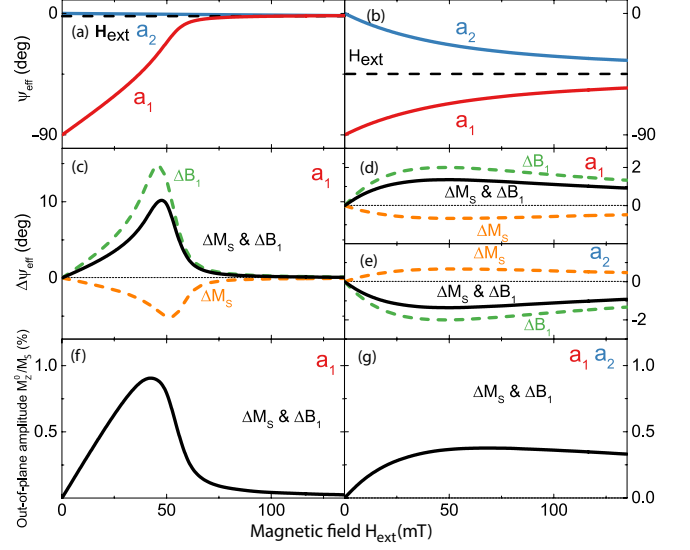


FIG. 2. (Color online) Calculated field dependencies of (a,b) the equilibrium effective field \mathbf{H}_{eff} orientation ψ_{eff} in the a_1 (red lines) and a_2 (blue lines) domains; and (c,d,e) its change $\Delta\psi_{\text{eff}}$ due to laser-induced demagnetization ΔM_S (orange dashed line), the change of magnetoelastic parameter ΔB_1 (green dashed line), and the total laser-induced effect (solid black line). (f,g) Calculated field dependence of the precession amplitude $\Delta M_z^0/M_S$ resulting from ΔM_S , ΔB_1 , and $\Delta u_{xx(yy)}$. The external field \mathbf{H}_{ext} is applied (a,c,f) at $\varphi = -1^\circ$ and (b,d,e,g) at $\varphi = -45^\circ$.

amorphous alloys [55, 56]. Then $\Delta B_1/B_1$ is estimated to be about -15% for the laser fluence of 10 mJ/cm^2 . The strains in the $a_1(a_2)$ domain change by $\Delta u_{xx}/u_{xx} \approx 19\%$ (-23%) and $\Delta u_{yy}/u_{yy} \approx 23\%$ (19%) for the ionic temperature increase of $\Delta T = 150 \text{ K}$ estimated for a laser fluence of 10 mJ/cm^2 (see Suppl. Mater.) using literature data on Au and CoFeB properties [57–60].

Figure 2 summarizes the results of the calculations for the a_1 and a_2 domains for the external magnetic field applied at $\varphi = -1^\circ$ and $\varphi = -45^\circ$ to the x axis. A misalignment $\varphi = -1^\circ$ was introduced to achieve better agreement between the measured and calculated field dependencies of the precession frequency, and is within the precision of field alignment in the experiments. An equilibrium RT magnetization $M_S = 0.85 \cdot 10^6 \text{ A/m}$ and magnetoelastic parameter $B_1 = -12.6 \cdot 10^5 \text{ mJ/cm}^3$ were used to obtain good agreement between the calculated and experimental field dependencies of the precession frequency [Fig. 1(e)]. The magnetoelastic anisotropy energy associated with the 90° in-plane magnetization rotation $B_1(u_{yy} - u_{xx}) = -2.17 \cdot 10^4 \text{ mJ/cm}^3$ and the magnetostriction coefficient $\lambda = 8 \cdot 10^{-6}$ agree with previous works considering similar systems [25, 61].

Figures 2(a-e) show the calculated field dependence of the equilibrium angle ψ_{eff} between \mathbf{H}_{eff} and the x axis and its change $\Delta\psi_{\text{eff}}$ under laser excitation. Four scenarios are modeled, taking into account ultrafast demagnetization ΔM_S only (orange dashed line), the decrease of the

magnetoelastic parameter ΔB_1 only (green dashed line), the change of strains Δu_{xx} and Δu_{yy} only (not shown), and the combination of all three (solid black line). As expected, ΔM_S and ΔB_1 result in opposite signs of $\Delta\psi_{\text{eff}}$. The effect of Δu_{xx} and Δu_{yy} appears to be considerably smaller than that of ΔM_S and ΔB_1 , in agreement with previous studies [62]. Indeed, the thermal expansion reduces the tensile in-plane strain and increases the compressive one, thus affecting the magnetoelastic energy weakly. If all effects are combined, the laser-induced decrease of the magnetoelastic parameter ΔB_1 governs the magnetization response. The reorientation of the total effective field is therefore dictated by a *decrease* of the in-plane magnetoelastic anisotropy field H_{ME} .

In our model, the precession of magnetization is excited, i.e. $\Delta\psi_{\text{eff}} \neq 0$, in the whole studied field range in both domains at $\varphi = -45^\circ$ and only at low fields in the a_1 domain at $\varphi = -1^\circ$ [Figs. 2(c-e)], which is in a good agreement with the experimental results [Fig. 1(f)]. The maximum absolute value of $\Delta\psi_{\text{eff}}$ is close to 10° if $\varphi = -1^\circ$, while it is several times smaller at $\varphi = -45^\circ$. Taking into account the strong ellipticity ϵ of the excited precession, which depends the applied field strength and orientation, we obtain a reasonable agreement between the calculated and experimental amplitudes of the precession $\Delta M_z^0/M_S$ [Figs. 1(f) and 2 (f,g)].

In the calculations we neglected effects on the laser-induced dynamics in a particular domain imposed by neighboring domains. This is justified by the experimental results showing that the frequencies of the excited precession in a_1 and a_2 domains at $\varphi = \pm 45^\circ$ are equal. Evident in Figs. 1(c,f), a difference in the precession amplitudes detected in the a_1 and a_2 domains at $\varphi = -45^\circ$ could originate from the fact that the width of the a_2 domain is somewhat smaller than the probe spot size. As a result, the probe averages the magnetization dynamics in the a_2 domain and in a part of the neighbouring a_1 domains, where the precession phase ξ_0 is opposite. This reduces the overall detected transient Kerr rotation. The effect is even more pronounced at $\varphi = 45^\circ$, where no precession signal from the a_2 domain is detected. In this case, the field is applied along the stripe domains, which initializes head-to-head and tail-to-tail domain walls having a width of about $1.5 \mu\text{m}$ [27]. As it is comparable to the width of the a_2 domain, the magnetization in the narrow a_2 domain is non-uniform, which suppresses the measured signal. For the wider a_1 domains or field orientations that initialize narrow head-to-tail domain walls, a similar reduction of the precession signal does not occur.

Our model successfully captures the main experimental findings with the only two fit parameters being the equilibrium values of M_S and B_1 . Their variation affects the absolute values of the precession frequency and effective anisotropy field, but not the characteristic features of the laser-driven magnetization precession. Therefore, our experiments unambiguously show that magnetoelastic anisotropy can be altered in a metallic film by ultrafast laser-induced heating similarly to magnetocrystalline

and growth-induced anisotropies [37, 39, 62]. In composite multiferroic and magnetoelectric structures, altering the magnetoelastic parameter of the FM constituent by laser excitation may lead to several specific phenomena. First, in our experiments the precession excited via a change of the magnetoelastic parameter enables distinguishing different types of domains in fields up to 120 mT. This is in contrast to static magneto-optical measurements, which only resolve domain structure in this geometry at much lower fields [25]. The higher sensitivity of the dynamical magneto-optical signal originates from the fact that magnetization at equilibrium approaches the direction of the external field at $\varphi = \pm 45^\circ$ asymptotically [Fig. 2(b)]. As a result, the condition $\Delta\psi_{\text{eff}} \neq 0$ for the precession excitation is fulfilled for each domain in a large field range, and the domains can be distinguished by opposite signs of $\Delta\psi_{\text{eff}}$ [Fig. 1(c)].

The possibility to alter the magnetoelastic parameter by laser pulses can be exploited further. A decrease of B_1 reduces the strain-mediated magnetoelectric coupling in multiferroic structures, which could enable laser-assisted magnetization switching with submicrometer spatial resolution [17]. Moreover, in strained films a spin reorientation transition can occur due to an extra contribution to the out-of-plane anisotropy (Eq. 1) controlled by the magnetoelastic parameter [40]. Hence, laser excitation may be used to trigger such a transition at picosecond timescale via changes of B_1 and film strains. Finally, laser-induced changes of magnetoelastic anisotropy may be employed for driving spin waves [63] in switchable magnonic waveguides based on CoFeB/BaTiO₃ [25, 27, 64, 65].

In conclusion, we have shown that the magnetoelastic coupling in a metallic CoFeB film can be significantly reduced on a picosecond timescale by excitation with a femtosecond laser pulse. This effect is explained by a simple model, which accounts for a laser-induced increase of electronic and ionic temperatures and relates the induced changes of the magnetoelastic parameter and magnetization via a $n(n+1)/2$ -law. This law appears to hold for laser-induced processes in metals at timescales beyond several picoseconds following excitation, which is required for establishing a quasi-equilibrium between the electronic, ionic and spin subsystems. The demonstrated ability to decrease the magnetoelastic parameter by laser pulses enables the driving of magnetization dynamics in metallic films wherein the magnetoelastic anisotropy dominates. We employed this mechanism to experimentally realize selective excitation of magnetization precession in individual micron-size magnetic stripe domains imprinted in a CoFeB film by a ferroelectric BaTiO₃ substrate. We found that the excitation of precession in an individual CoFeB domain is controlled by the strength and the orientation of the applied magnetic field with respect to the local uniaxial anisotropy axis, which allows distinguishing magnetization precessions in separate domains even when they are unresolvable in static measurements due to large applied magnetic field.

We thank N. E. Khokhlov and P. I. Gerevenkov for the fruitful discussions. TEM study was carried out using Jeol JEM-2100F microscope of the Federal Joint Research Center "Materials science and characterization in advanced technologies". L.A.Sh., A.V.Sch. and A.M.K. acknowledge RSF (grant No. 16-12-10485) for the support of the experimental studies, and the RFBR (grant No. 19-

52-12065) and the DFG programme TRR160 ICRC for the support of the theoretical work. S.J.H. and S.v.D. were supported by the Academy of Finland (grant No. 316857). Collaboration between the Ioffe Institute and Aalto University is a part of the COST Action CA17123 Magnetofon.

-
- * shelukhin@mail.ioffe.ru
- ¹ G. A. Smolenskii and I. E. Chupis, "Ferroelectromagnets," *Sov. Phys.: Uspekhi* **25**, 475–493 (1982).
 - ² M. Fiebig, "Revival of the magnetoelectric effect," *J. Phys. D: Appl. Phys.* **38**, R123–R152 (2005).
 - ³ J.-M. Hu, L.-Q. Chen, and C.-W. Nan, "Multiferroic heterostructures integrating ferroelectric and magnetic materials," *Adv. Mater.* **28**, 15–39 (2015).
 - ⁴ S. Manipatruni, D. E. Nikonov, C.-C. Lin, T. A. Gosavi, H. Liu, B. Prasad, Y.-L. Huang, E. Bonturim, R. Ramesh, and I. A. Young, "Scalable energy-efficient magnetoelectric spinorbit logic," *Nature* **565**, 35 (2019).
 - ⁵ Z. Chu, M. PourhosseiniAsl, and S. Dong, "Review of multi-layered magnetoelectric composite materials and devices applications," *J. Phys. D: Appl. Phys.* **51**, 243001 (2018).
 - ⁶ N. A. Hill, "Why are there so few magnetic ferroelectrics?" *J. Phys. Chem. B* **104**, 6694–6709 (2000).
 - ⁷ C. A. F. Vaz, "Electric field control of magnetism in multiferroic heterostructures," *J. Phys. Condens. Matter* **24**, 333201 (2012).
 - ⁸ Y. Wang, J. Hu, Y. Lin, and C.-W. Nan, "Multiferroic magnetoelectric composite nanostructures," *NPG Asia Mater.* **2**, 61–68 (2010).
 - ⁹ G. P. Carman and N. Sun, "Strain-mediated magnetoelectrics: Turning science fiction into reality," *MRS Bull.* **43**, 822–828 (2018).
 - ¹⁰ C.-W. Nan, M. I. Bichurin, S. Dong, D. Viehland, and G. Srinivasan, "Multiferroic magnetoelectric composites: Historical perspective, status, and future directions," *J. Appl. Phys.* **103**, 031101 (2008).
 - ¹¹ T. Taniyama, K. Akasaka, D. Fu, M. Itoh, H. Takashima, and B. Prijamboedi, "Electrical voltage manipulation of ferromagnetic microdomain structures in a ferromagnetic/ferroelectric hybrid structure," *J. Appl. Phys.* **101**, 09F512 (2007).
 - ¹² T. H. E. Lahtinen, J. O. Tuomi, and S. van Dijken, "Pattern transfer and electric-field-induced magnetic domain formation in multiferroic heterostructures," *Adv. Mater.* **23**, 3187–3191 (2013).
 - ¹³ Y. Shirahata, R. Shiina, D. L. González, K. J. A. Franke, E. Wada, M. Itoh, N. A. Pertsev, S. van Dijken, and T. Taniyama, "Electric-field switching of perpendicularly magnetized multilayers," *NPG Asia Mater.* **7**, e198 (2015).
 - ¹⁴ T. H. E. Lahtinen, K. J. A. Franke, and S. Van Dijken, "Electric-field control of magnetic domain wall motion and local magnetization reversal," *Sci. Rep.* **2**, 258 (2012).
 - ¹⁵ M. Buzzi, R. V. Chopdekar, J. L. Hockel, A. Bur, T. Wu, N. Pilet, P. Warnicke, G. P. Carman, L. J. Heyderman, and F. Nolting, "Single domain spin manipulation by electric fields in strain coupled artificial multiferroic nanostructures," *Phys. Rev. Lett.* **111**, 027204 (2013).
 - ¹⁶ K. J. A. Franke, B. Van de Wiele, Y. Shirahata, S. J. Hämmäläinen, T. Taniyama, and S. van Dijken, "Reversible electric-field-driven magnetic domain-wall motion," *Phys. Rev. X* **5**, 011010 (2015).
 - ¹⁷ R. L. Conte, J. Gorchon, A. Mougin, C. H. A. Lambert, A. El-Ghazaly, A. Scholl, S. Salahuddin, and J. Bokor, "Electrically controlled switching of the magnetization state in multiferroic BaTiO₃/CoFe submicrometer structures," *Phys. Rev. Mater.* **2**, 091402 (2018).
 - ¹⁸ C. Cavaco, M. Van Kampen, L. Lagae, and G. Borghs, "A room-temperature electrical field-controlled magnetic memory cell," *J. Mater. Res.* **22**, 2111–2115 (2007).
 - ¹⁹ N. A. Pertsev and H. Kohlstedt, "Magnetic tunnel junction on a ferroelectric substrate," *Appl. Phys. Lett.* **95**, 163503 (2009).
 - ²⁰ N. A. Pertsev and H. Kohlstedt, "Resistive switching via the converse magnetoelectric effect in ferromagnetic multilayers on ferroelectric substrates," *Nanotechnology* **21**, 475202 (2010).
 - ²¹ M. Liu, S. Li, O. Obi, J. Lou, S. Rand, and N. X. Sun, "Electric field modulation of magnetoresistance in multiferroic heterostructures for ultralow power electronics," *Appl. Phys. Lett.* **98**, 222509 (2011).
 - ²² A. Chen, Y. Wen, B. Fang, Y. Zhao, Q. Zhang, Y. Chang, P. Li, H. Wu, H. Huang, Y. Lu, Z. Zeng, J. Cai, X. Han, T. Wu, X.-X. Zhang, and Y. Zhao, "Giant nonvolatile manipulation of magnetoresistance in magnetic tunnel junctions by electric fields via magnetoelectric coupling," *Nat. Commun.* **10**, 1–7 (2019).
 - ²³ M. Liu, Z. Zhou, T. Nan, B. M. Howe, G. J. Brown, and N. X. Sun, "Voltage tuning of ferromagnetic resonance with bistable magnetization switching in energy-efficient magnetoelectric composites," *Adv. Mater.* **25**, 1435–1439 (2013).
 - ²⁴ J. Lou, M. Liu, D. Reed, Y. Ren, and N. X. Sun, "Giant electric field tuning of magnetism in novel multiferroic FeGaB/lead zinc niobate/lead titanate (PZN-PT) heterostructures," *Adv. Mater.* **21**, 4711–4715 (2009).
 - ²⁵ F. Brandl, K. J. A. Franke, T. H. E. Lahtinen, S. van Dijken, and D. Grundler, "Spin waves in CoFeB on ferroelectric domains combining spin mechanics and magnonics," *Solid State Commun.* **198**, 13–17 (2014).
 - ²⁶ A. V. Azovtsev and N. A. Pertsev, "Electrical tuning of ferromagnetic resonance in thin-film nanomagnets coupled to piezoelectrically active substrates," *Phys. Rev. Appl.* **10**, 044041 (2018).
 - ²⁷ S. J. Hämmäläinen, M. Madami, H. Qin, G. Gubbiotti, and S. van Dijken, "Control of spin-wave transmission by a programmable domain wall," *Nat. Commun.* **9**, 1–8 (2018).
 - ²⁸ A. V. Sadovnikov, A. A. Grachev, S. E. Sheshukova, Yu. P. Sharaevskii, A. A. Serdobintsev, D. M. Mitin, and S. A. Nikitov, "Magnon straintronics: reconfigurable spin-wave

- routing in strain-controlled bilateral magnetic stripes,” *Phys. Rev. Lett.* **120**, 257203 (2018).
- ²⁹ E. O. Savostin and N. A. Pertsev, “Superconducting straintronics via the proximity effect in superconductor–ferromagnet nanostructures,” *Nanoscale* **12**, 648–657 (2020).
 - ³⁰ A. Kirilyuk, A. V. Kimel, and Th. Rasing, “Ultrafast optical manipulation of magnetic order,” *Rev. Mod. Phys.* **82**, 2731–2784 (2010).
 - ³¹ Y. M. Sheu, S. A. Trugman, L. Yan, Q. X. Jia, A. J. Taylor, and R. P. Prasankumar, “Using ultrashort optical pulses to couple ferroelectric and ferromagnetic order in an oxide heterostructure,” *Nat. Commun.* **5**, 1–6 (2014).
 - ³² C. Jia, N. Zhang, A. Sukhov, and J. Berakdar, “Ultrafast transient dynamics in composite multiferroics,” *New J. Phys.* **18**, 023002 (2016).
 - ³³ M. Lejman, G. Vaudel, I. C. Infante, P. Gemeiner, V. E. Gusev, B. Dkhil, and P. Ruello, “Giant ultrafast photo-induced shear strain in ferroelectric BiFeO₃,” *Nat. Commun.* **5**, 1–7 (2014).
 - ³⁴ A. V. Kimel, A. M. Kalashnikova, A. Pogrebna, and A. K. Zvezdin, “Fundamentals and perspectives of ultrafast photoferroic recording,” *Phys. Rep.* (2020), <https://doi.org/10.1016/j.physrep.2020.01.004>.
 - ³⁵ H.-J. Liu, L.-Y. Chen, Q. He, C.-W. Liang, Y.-Z. Chen, Y.-S. Chien, Y.-H. Hsieh, S.-J. Lin, E. Arenholz, C.-W. Luo, Y.-L. Chueh, Y.-C. Chen, and Y.-H. Chu, “Epitaxial photostrictionmagnetostriction coupled self-assembled nanostructures,” *ACS Nano* **6**, 6952–6959 (2012).
 - ³⁶ J.-Y. Bigot, M. Vomir, L. H. F. Andrade, and E. Beaupaire, “Ultrafast magnetization dynamics in ferromagnetic cobalt: The role of the anisotropy,” *Chem. Phys.* **318**, 137–146 (2005).
 - ³⁷ E. Carpenne, E. Mancini, D. Dazzi, C. Dallera, E. Puppini, and S. De Silvestri, “Ultrafast three-dimensional magnetization precession and magnetic anisotropy of a photoexcited thin film of iron,” *Phys. Rev. B* **81**, 060415 (2010).
 - ³⁸ E. Carpenne, E. Mancini, C. Dallera, E. Puppini, and S. De Silvestri, “Three-dimensional magnetization evolution and the role of anisotropies in thin Fe/MgO films: Static and dynamic measurements,” *J. Appl. Phys.* **108**, 063919 (2010).
 - ³⁹ L. A. Shelukhin, V. V. Pavlov, P. A. Usachev, P. Yu. Shamray, R. V. Pisarev, and A. M. Kalashnikova, “Ultrafast laser-induced changes of the magnetic anisotropy in a low-symmetry iron garnet film,” *Phys. Rev. B* **97**, 014422 (2018).
 - ⁴⁰ N. A. Pertsev, “Giant magnetoelectric effect via strain-induced spin reorientation transitions in ferromagnetic films,” *Phys. Rev. B* **78**, 212102 (2008).
 - ⁴¹ J. P. Hirth and J. Lothe, *Theory of Dislocations* (McGraw-Hill, New York, 1968).
 - ⁴² Y. S. Touloukian, R. W. Powell, C. Y. Ho, and P. G. Klemens, “Thermophysical properties of matter—the tprc data series. volume 2. thermal conductivity-nonmetallic solids,” IFI/Plenum, New York (1970).
 - ⁴³ K. An, X. Ma, C.-F. Pai, J. Yang, K. S. Olsson, J. L. Erskine, D. C. Ralph, R. A. Buhrman, and X. Li, “Current control of magnetic anisotropy via stress in a ferromagnetic metal waveguide,” *Phys. Rev. B* **93**, 140404 (2016).
 - ⁴⁴ “BaTiO₃ crystal structure: Datasheet from “PAULING FILE Multinaries Edition – 2012” in SpringerMaterials.”
 - ⁴⁵ H. F. Kay and P. Vousden, “Xcv. symmetry changes in barium titanate at low temperatures and their relation to its ferroelectric properties,” *Philos. Mag.* **40**, 1019–1040 (1949).
 - ⁴⁶ E. Beaupaire, J.-C. Merle, A. Daunois, and J.-Y. Bigot, “Ultrafast spin dynamics in ferromagnetic nickel,” *Phys. Rev. Lett.* **76**, 4250–4253 (1996).
 - ⁴⁷ B. Koopmans, G. Malinowski, F. Dalla Longa, D. Steiauf, M. Fähnle, T. Roth, M. Cinchetti, and M. Aeschlimann, “Explaining the paradoxical diversity of ultrafast laser-induced demagnetization,” *Nat. Mater.* **9**, 259–265 (2010).
 - ⁴⁸ M. van Kampen, C. Jozsa, J. T. Kohlhepp, P. LeClair, L. Lagae, W. J. M. de Jonge, and B. Koopmans, “All-optical probe of coherent spin waves,” *Phys. Rev. Lett.* **88**, 227201 (2002).
 - ⁴⁹ J. Smit and H. G. Beljers, “Ferromagnetic resonance absorption in BaFe₁₂O₁₉ a highly anisotropic crystal,” *Philips Res. Repts* **10** (1955).
 - ⁵⁰ H. Suhl, “Ferromagnetic resonance in nickel ferrite between one and two kilomegacycles,” *Phys. Rev.* **97**, 555–557 (1955).
 - ⁵¹ A. G. Gurevich and G. A. Melkov, *Magnetization oscillations and waves* (CRC press, 1996).
 - ⁵² E. R. Callen and H. B. Callen, “Anisotropic magnetization,” *J. Phys. Chem. Solids* **16**, 310 – 328 (1960).
 - ⁵³ C. Kittel and J. H. Van Vleck, “Theory of the temperature dependence of the magnetoelastic constants of cubic crystals,” *Phys. Rev.* **118**, 1231–1232 (1960).
 - ⁵⁴ E. Callen and H. B. Callen, “Magnetostriction, forced magnetostriction, and anomalous thermal expansion in ferromagnets,” *Phys. Rev.* **139**, A455–A471 (1965).
 - ⁵⁵ R. C. O’Handley, “Temperature dependence of magnetostriction in Fe₈₀B₂₀ glass,” *Solid State Commun.* **22**, 485 – 488 (1977).
 - ⁵⁶ J. M. Barandiarán, J. Gutiérrez, and A. García-Arribas, “Magneto-elasticity in amorphous ferromagnets: Basic principles and applications,” *phys. status solidi (a)* **208**, 2258–2264 (2011).
 - ⁵⁷ M. Walter, J. Walowski, V. Zbarsky, M. Münzenberg, M. Schäfers, D. Ebke, G. Reiss, A. Thomas, P. Peretzki, M. Seibt, J. S. Moodera, M. Czerner, M. Bachmann, and C. Heiliger, “Seebeck effect in magnetic tunnel junctions,” *Nat. Mater.* **10**, 742 (2011).
 - ⁵⁸ C.-Y. Liang, A. E. Sepulveda, D. Hoff, S. M. Keller, and G. P. Carman, “Strain-mediated deterministic control of 360 domain wall motion in magnetoelastic nanorings,” *J. Appl. Phys.* **118**, 174101 (2015).
 - ⁵⁹ P. B. Johnson and R. W. Christy, “Optical constants of the noble metals,” *Phys. Rev. B* **6**, 4370–4379 (1972).
 - ⁶⁰ R. C. O’Handley, R. Hasegawa, R. Ray, and C.-P. Chou, “Ferromagnetic properties of some new metallic glasses,” *Appl. Phys. Lett.* **29**, 330–332 (1976).
 - ⁶¹ S. Isogami and T. Taniyama, “Strain mediated in-plane uniaxial magnetic anisotropy in amorphous CoFeB films based on structural phase transitions of BaTiO₃ single-crystal substrates,” *phys. status solidi (a)* **215**, 1700762 (2018).
 - ⁶² V. N. Kats, T. L. Linnik, A. S. Salasyuk, A. W. Rushforth, M. Wang, P. Wadley, A. V. Akimov, S. A. Cavill, V. Holy, A. M. Kalashnikova, and A. V. Scherbakov, “Ultrafast changes of magnetic anisotropy driven by laser-generated coherent and noncoherent phonons in metallic films,” *Phys. Rev. B* **93**, 214422 (2016).
 - ⁶³ N. E. Khokhlov, P. I. Gerevenkov, L. A. Shelukhin, A. V. Azovtsev, N. A. Pertsev, M. Wang, A. W. Rushforth, A. V. Scherbakov, and A. M. Kalashnikova, “Optical excitation

of propagating magnetostatic waves in an epitaxial galferol film by ultrafast magnetic anisotropy change,” *Phys. Rev. Appl.* **12**, 044044 (2019).

- ⁶⁴ B. Van de Wiele, S. J. Hämäläinen, P. Baláž, F. Montoncello, and S. Van Dijken, “Tunable short-wavelength spin wave excitation from pinned magnetic domain walls,” *Sci.*

Rep. **6**, 21330 (2016).

- ⁶⁵ D. López González, A. Casiraghi, B. Van de Wiele, and S. Van Dijken, “Reconfigurable magnetic logic based on the energetics of pinned domain walls,” *Appl. Phys. Lett.* **108**, 032402 (2016).

Supplementary Material

Laser-induced magnetization precession in individual magnetoelastic domains of a multiferroic CoFeB/BaTiO₃ composite

L. A. Shelukhin,^{1,*} N. A. Pertsev,¹ A. V. Scherbakov,^{1,2} D. L. Kazenwadel,³
D. A. Kirilenko,¹ S. J. Härmäläinen,⁴ S. van Dijken,⁴ and A. M. Kalashnikova¹

¹*Ioffe Institute, 194021 St. Petersburg, Russia*

²*Experimental Physics II, Technical University Dortmund, D-44227 Dortmund, Germany*

³*University of Konstanz, D-78457 Konstanz, Germany*

⁴*NanoSpin, Department of Applied Physics, Aalto University School of Science, P.O. Box 15100, FI-00076 Aalto, Finland*
(Dated: March 26, 2025)

I. TRANSMISSION ELECTRON MICROSCOPY

Figure 1 shows the transmission electron microscopy (TEM) images of the CoFeB/BaTiO₃ heterostructure. Cross-section TEM specimen were prepared by mechanical polishing with subsequent ion milling by Ar⁺@3 keV. A Jeol JEM-2100F microscope operated at 200 kV was used to acquire images in conventional bright-field and high-resolution modes. The CoFeB film is amorphous with a short-range order present at lengthscale of ~ 1 nm.

II. RAW PUMP-PROBE DATA

Figure 2 shows raw pump-probe data, used to obtain Figs. 1(c,d) in the main text. Slow varying background seen in Fig. 2 is of nonmagnetic origin and, thus, has been subtracted from the data in Figs. 1(c,d) of the main text, for the sake of clarity.

III. ULTRAFAST LASER-INDUCED HEATING

For the estimation of ultrafast temperature change in the ferromagnetic layer in CoFeB/BaTiO₃ under influence of femtosecond laser pulses we used the following parameters. Pump with wavelength 515 nm has fluence 10 mJ/cm². The refractive index n and extinction coefficient k of the capping gold layer with thickness 6 nm amount 0.72 and 2.02, respectively [1]. This gives transmission $T_{\text{Au}}=0.74$ and reflection coefficient on the interface gold-air $R_{\text{air-Au}}=0.6$. The refractive index n and extinction coefficient k of the 50 nm CoFeB layer are 2.5 and 3.3, respectively [2] which gives reflection coefficient on the interface with gold $R_{\text{Au-CoFeB}}=0.27$. Taking CoFeB heat capacity $C_{\text{CoFeB}}=440 \text{ J kg}^{-1}\text{K}^{-1}$ [3] and density $\rho=7.7\cdot 10^3 \text{ kg m}^{-3}$ [4] one gets heating of $\Delta T \sim 150 \text{ K}$.

* shelukhin@mail.ioffe.ru

¹ P. B. Johnson and R. W. Christy, "Optical constants of the noble metals," Phys. Rev. B **6**, 4370–4379 (1972).

² X. Liang, X. Xu, R. Zheng, Z. A. Lum, and J. Qiu, "Optical constant of CoFeB thin film measured with the interference enhancement method," Appl. Opt. **54**, 1557–1563 (2015).

³ M. Walter, J. Walowski, V. Zbarsky, M. Münzenberg, M. Schäfers, D. Ebke, G. Reiss, A. Thomas, P. Peretzki, M. Seibt, J. S. Moodera, M. Czerner, M. Bachmann, and C. Heiliger, "Seebeck effect in magnetic tunnel junctions," Nat. Mater. **10**, 742 (2011).

⁴ R. C. O'Handley, R. Hasegawa, R. Ray, and C.-P. Chou, "Ferromagnetic properties of some new metallic glasses," Appl. Phys. Lett. **29**, 330–332 (1976).

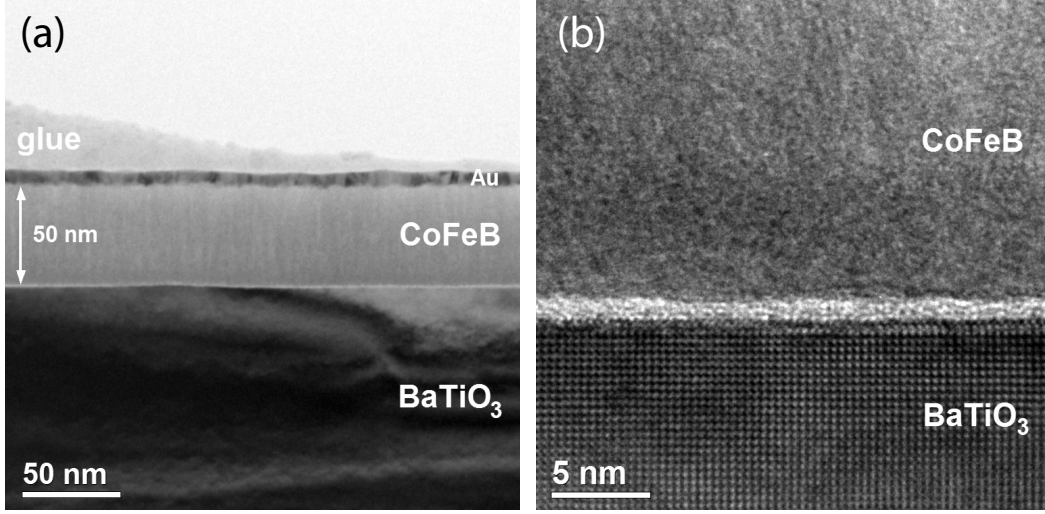


FIG. 1. Bright-field (a) and high-resolution (b) TEM images of the CoFeB/BaTiO₃ heterostructure.

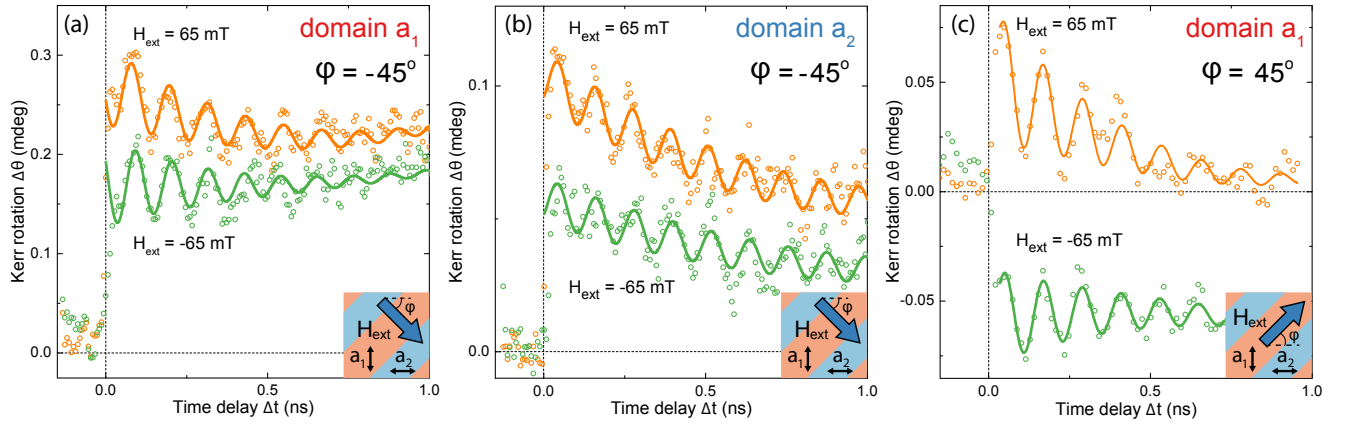


FIG. 2. (Color online) (a, b) Laser-induced Kerr rotation of the probe pulse polarization plane as a function of time delay Δt measured in a_1 (a) and a_2 (b) domain for $H_{\text{ext}}=65$ mT (orange) and -65 mT (green) directed at $\varphi=-45^\circ$ (magnetic field is perpendicular to the domain wall). (c) Laser-induced Kerr rotation of the probe pulse polarization plane as a function of time delay Δt measured in a_1 domain for $H_{\text{ext}}=65$ mT (top) and -65 mT (bottom) directed at $\varphi=45^\circ$ (magnetic field is parallel to the domain walls). Dots is experiment, solid lines are fit (see main text). Insets schematically depicts direction of the easy axis in domains and external field.